Interaction between HfC precipitates and vacancies in quenched Cu:Hf as studied by TDPAC and positron lifetime measurements

2004 J. Phys.: Condens. Matter 16 6579

(http://iopscience.iop.org/0953-8984/16/36/023)

INSTITUTE OF PHYSICS PUBLISHING JOURNAL OF PHYSICS: CONDENSED MATTER

J. Phys.: Condens. Matter **16** (2004) 6579–6588 PII: S0953-8984(04)76043-9

Interaction between HfC precipitates and vacancies in quenched Cu:Hf as studied by TDPAC and positron lifetime measurements

R Govindaraj and R Rajaraman

Materials Science Division, Indira Gandhi Centre for Atomic Research, Kalpakkam-603 102, India

E-mail: govind@igcar.ernet.in

Received 11 February 2004
Published 27 August 2004
Online at stacks.iop.org/JPhysCM/16/6579
doi:10.1088/0953-8984/16/36/023

Abstract

A Cu:Hf sample with 1 wt% Hf as prepared by arc melting is characterized by TEM and microdiffraction analysis to contain HfC precipitates. HfC precipitates in a Cu matrix bind vacancies and divacancies strongly in the quenched Cu:Hf sample as deduced by time differential perturbed angular correlation (TDPAC) studies. Isochronal annealing studies using TDPAC and positron lifetime measurements indicate the stability of these vacancy complexes in the quenched sample for annealing treatments up to 1200 K, beyond which the de-trapping of the vacancies from HfC precipitates is observed to occur. This shows that HfC precipitates present in Cu inhibit the formation of voids by strongly binding quenched vacancies.

1. Introduction

Knowledge of the interaction of solute atoms with vacancies in metals is of fundamental importance for understanding the results of annealing, quenching and diffusion experiments [1]. In many cases non-equilibrium treatments of metallic alloys such as irradiation, quenching and cold-working lead to an occurrence of lattice coherent aggregates, namely solute-rich clusters, Guinier–Preston zones and precipitates [2, 3]. The presence of low concentrations of vacancies and fine granular precipitates/solute clusters leads to the enhancement of mechanical strength by means of inhibiting dislocation motion [4, 5]. Therefore it becomes pertinent to study the interaction between solute clusters and lattice defects in detail. In a number of cases, solute atoms and their clusters bind vacancies quite strongly. The solute atom–vacancy interaction can be studied intensively using microscopic techniques such as time differential perturbed angular correlation (TDPAC) [6, 7] and positron annihilation spectroscopies [8, 9]. Hf solute

clusters are observed to bind vacancies and helium associated vacancy complexes strongly in helium implanted Cu:Hf and Al:Hf by TDPAC and positron lifetime measurements [10, 11].

In the present study the reference Cu:Hf sample is characterized by TEM and microdiffraction analysis to contain HfC precipitates as will be discussed in the results and discussion section. Large hardness, high melting point and wear resistance are the key properties for the technological applications of carbides and nitrides of transition metals to cutting tools and hard coatings. The interaction between metallic carbides and vacancies is of technological importance as the metallic carbides are highly resistant to void swelling [12–14]. It is also of interest in view of corrosion and precipitate strengthening and to reduce helium embrittlement [15, 16]. On the other hand not many detailed studies have been carried out on the interaction between HfC precipitates and vacancies in different matrices. The present work is aimed at studying the interaction between HfC solute clusters and vacancies in a Cu:Hf matrix by TDPAC and positron lifetime measurements. The merits and demerits of these techniques are discussed in a detailed manner in the following paragraph in view of combining them to address the problem concerned.

TDPAC is a hyperfine interaction technique and is a sensitive method in studying the point defects in metals as they probe the formation of impurity–point defect complexes on a microscopic scale [17, 18]. The diffusing defects which migrate and trap next to the radioactive probe nuclei during the annealing treatment of the sample are detected through the interaction of the nuclear moments of the probe nuclei with the electro-magnetic fields in their nearest neighbouring environment. The change of microscopic structure of the lattice due to a defect produces changes in the local electron density distribution which results in the occurrence of electric field gradient (EFG) at the probe nucleus in a diamagnetic fcc matrix [18]. Since the EFG at the probe nucleus varies inversely as the cube of the distance between the defect and the probe atom, its absolute value rapidly decreases with increasing distance from the defect. Therefore, the defects which are bound to the probe atoms alone can be detected by TDPAC. Hence based on annealing measurements it is possible to deduce probe–defect binding energy. However, if the configuration of vacancy clusters as bound to probe atoms in Cu is of cubic symmetry, it cannot be detected by TDPAC as the defect–probe complex is configured by a zero electric field gradient and hence no quadrupole interaction. Cubic vacancy clusters bound to the probe atom in a magnetically ordered host could however be detected, due to a distinct magnetic interaction as experienced by the probe atoms. Vacancy clusters, whether isolated or bound to any impurity atom, can be detected very well by positron lifetime measurements. Positron lifetime is quite sensitive to local electron density at the annihilation site. Strong trapping of positrons at vacancy type defects makes this technique a selective and sensitive tool to study vacancies and their clusters. The lifetime of the positrons is sensitively dependent upon the size of the vacancy clusters and their concentration [19]. But the positron lifetime measurements give no information on the chemical surroundings and hence cannot identify the sublattice of the vacancy or whether the vacancy is isolated or forms a complex with impurity atoms. Vacancy–solute interactions can indirectly be studied by positron lifetime measurements based on a comparison of the results in terms of onset of defect migration, annealing etc with those obtained in pure material (free from solutes) subjected to identical non-equilibrium treatment [10]. The problem of vacancy–impurity interaction can be addressed well using coincident Doppler broadening measurements of the positron annihilated 511 keV γ rays [20]. It is possible to deduce the geometry of vacancy–probe complexes by TDPAC [18], while positron based techniques are not sensitive to deduce this information. Interaction between interstitial impurities and the probe atoms can also be studied by TDPAC [17], while interstitials cannot be studied by positron annihilation spectroscopy due to electrostatic repulsive interaction between positron and interstitials. Based on the above

points it can be inferred that the combination of TDPAC and positron lifetime techniques is quite powerful to address the problem of impurity–vacancy binding. Thus using these techniques a detailed study has been carried out on exploring the possible interaction between HfC and vacancies in quenched Cu:Hf containing HfC solute clusters.

2. Experimental details

An alloy of Cu (99.99% purity) with 1 wt% Hf (98.7% purity) has been prepared by arc melting. To ensure a better homogenization of the alloy, the resultant melt is cut into pieces and remelted. Finally, these melts are annealed at 1273 K for 96 h at 10^{-6} Torr. This is different from the homogenization procedure employed for Cu:Hf samples prepared earlier,[1] in which we have reported the effect of cold working on hafnium solute clusters by TDPAC and positron lifetime measurements [21]. Samples of dimensions $1 \times 0.1 \times 0.028$ and $1 \times 1 \times 0.028$ cm^3 are drawn from the melt by cold working and are annealed at 1273 K for 6 h at 10^{-6} Torr, to obtain the reference samples for TDPAC and positron lifetime measurements respectively. Detailed microstructural and microchemical investigations were carried out by transmission electron microscopy on thin foils, using a CM200 Philips Analytical Transmission Electron Microscope with SUTW Energy Dispersive Spectroscopy detector and DX4 Analyser. In this measurement TEM was operated at 200 kV. The resolution of TEM is about 4 Å.

The samples meant for TDPAC measurements were irradiated with thermal neutrons at the CIRUS reactor, Bhabha Atomic Research Centre, Mumbai, to a fluence of 2×10^{21} n m^{-2}, to produce ^{181}Ta probe nuclei by the reaction ^{180}Hf (n, γ) ^{181}Hf $\rightarrow^{\beta^-}$ ^{181}Ta. The TDPAC of the 133–482 keV γ–γ cascade of ^{181}Ta was measured by a three-detector twin fast–slow coincidence set-up using NaI(Tl) detectors. The prompt time resolution of the set-up measured with a ^{60}Co source was 2.2 ns FWHM when gated for the above cascade of ^{181}Ta [21]. One of the detectors is set for the first γ ray of the cascade (133 keV) and the other two detectors, located at 90° and 180° respectively with respect to the first one, are set to detect the second γ ray (482 keV) of the cascade. From the time delayed coincidence spectra $W(90°, t)$ and $W(180°, t)$, the anisotropy function, namely $R(t) = 2[W(180°, t) - W(90°, t)]/[W(180°, t) + 2W(90°, t)]$, has been deduced. The details of the data acquisition, deduction of the normalized anisotropy function $R(t)$ for various detector geometries are described for example in [22]. The normalized anisotropy $R(t)$ spectra were least squares fitted to the perturbation function $R(t) = A_2 \sum_{i=0}^{n} G_2^i(t)$. The value of n is determined by the number of resolved frequency components in the Fourier spectra $P(\omega)$ of the $R(t)$ spectrum. The perturbation function is given as $G_2^i(t) = \sum_{n=0}^{3} a_m^i \exp[-\delta_i k_m(\eta_i)\omega_{Qi} t] \cos[k_m(\eta_i)\omega_{Qi} t]$ with $\sum_{i=0}^{n} f_i = 1$, $\sum_{m=0}^{3} a_m^i(\eta_i) = 1$ [22, 23] to deduce the quadrupole parameters, namely the quadrupole frequency, $\nu_{Qi} = eQV_{zz}^i/h = 10\omega_{Qi}/3\pi$, where V_{zz} is the principal component of the electric field gradient (EFG) tensor. When the EFG is not axially symmetric, the asymmetry parameter $\eta = (V_{xx} - V_{yy})/V_{zz}$ where $|V_{zz}| \geqslant |V_{yy}| \geqslant |V_{xx}|$ is extracted from the fit of $R(t)$ data to equation (2). A non-vanishing value of δ (i.e. the width of the Lorentzian distribution of quadrupole frequency ν_Q) implies either a significant concentration of defects or a disordered arrangement of atoms in the probe surroundings.

Positron lifetime measurements were carried out using a fast–fast coincidence spectrometer with a time resolution of 240 ps (FWHM) [24]. The instrumental resolution and source annihilation parameters are evaluated from the RESOLUTION [25] fit. The

[1] Cu:Hf melts obtained after arc melting were sealed in a quartz tube at argon atmosphere and annealed for six days at 1200 K. This is the homogenization proceedure employed for the Cu:Hf sample prepared earlier [10] and is different from that of the present sample.

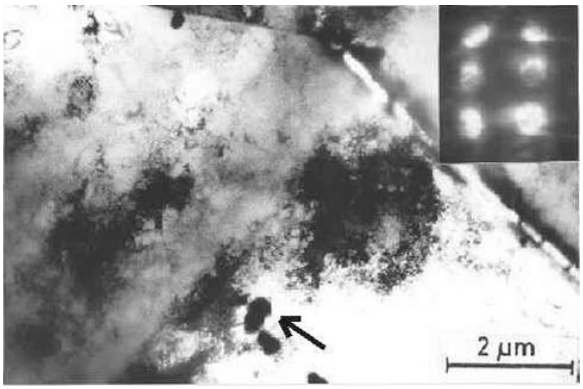

Figure 1. TEM micrograph showing the presence of HfC precipitate in reference Cu:Hf sample. The inset shows a microdiffraction pattern taken on the precipitate along $\langle 01\bar{1}\rangle$.

analysis of the lifetime spectrum is carried out using POSITRONFIT [25] to deduce lifetime components. As the present case may involve the binding of vacancy clusters by precipitates of different sizes there is also expected to be a distribution in the electron charge density at these precipitates and hence in positron lifetime. The distribution of annihilation rates $C(t)$ is given as $C(t) = \int_0^\infty \lambda\alpha(\lambda)\mathrm{e}^{-\lambda t}\,\mathrm{d}\lambda$. Here $C(t)$ is the Laplace transform of $\lambda\alpha(\lambda)$ and $\alpha(\lambda)$ is the annihilation rate probability distribution function. The fraction of positrons annihilating with rates between λ and $\lambda + \mathrm{d}\lambda$ is given as $\lambda\alpha(\lambda)$, which can be recovered by the inverse Laplace transform of $C(t)$ by CONTIN analysis [26].

TDPAC and positron lifetime measurements were made at room temperature on the respective samples quenched from 1323 K at a pressure of 10^{-6} Torr. Subsequent measurements were carried out at room temperature after each isochronal annealing treatment of the samples, with a step duration of 30 min.

3. Results and discussion

The TEM micrograph as shown in figure 1 indicates the presence of precipitates as marked by an arrow. The inset in the figure shows the microdiffraction pattern taken on the precipitate. The analysis of the microdiffraction pattern taken along $\langle 01\bar{1}\rangle$ confirms that the observed precipitate is HfC, based on the finding that the observed lattice structure (fcc) and the derived lattice parameter (4.64 Å) match with those of HfC. The presence of HfC precipitates in the samples is understood to be due to carbon contamination resulting from the diffusion pump of the vacuum system coupled to the arc furnace. Decomposition of hydrocarbons in the diffusion pump oil produces mainly carbon monoxide contaminants. When there is a backstreaming or evaporation of the diffusion pump oil into the vacuum system the contamination would be severe. This has resulted in the formation of HfC precipitates while arc melting or during homogenization of the melts by prolonged annealing at 1×10^{-6} Torr. Ni:Hf samples prepared under similar conditions using the same arc-melting and annealing systems are also characterized by TEM and SAD to contain HfC precipitates as reported [27].

The fitted time dependent anisotropy spectrum $R(t)$ and the corresponding Fourier transform $P(\omega)$ as obtained in the reference sample are shown in figure 2(a). The resultant hyperfine parameters corresponding to the reference sample are shown in table 1. The fraction f_0 is due to probe atoms occupying substitutional sites in the sample. An appreciable width

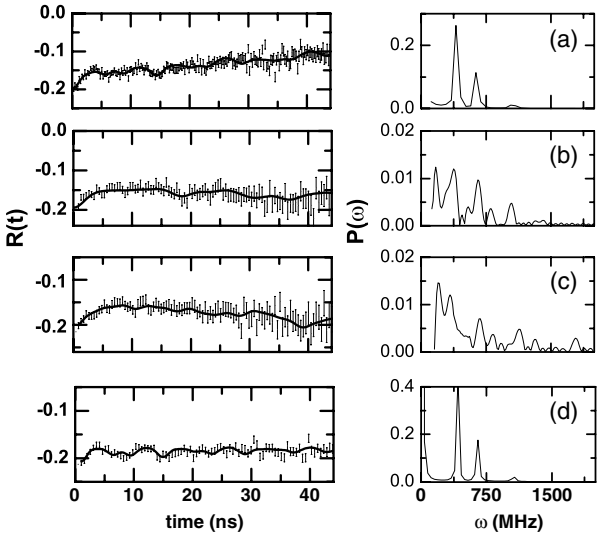

Figure 2. The TDPAC spectra ($R(t)$) in the Cu:Hf sample as obtained at room temperature, subjected to the following annealing treatments. (a) Reference sample; (b) as quenched; (c) $T_a = 600$ K and (d) $T_a = 1300$ K. The inset in (a) represents the Fourier transform $P(\omega)$ of the TDPAC spectrum of the reference sample.

Table 1. TDPAC and positron lifetime parameters and their assignments.

Experiment	Sample	Deduced resultant parameters	Assignments
TDPAC	Reference Cu:Hf	$f_0 = 0.71 \pm 0.05$, $\langle \nu_0 \rangle = 0$, $\delta\nu_0 = 2.8$ MHz	Probe atoms occupying substitutional sites
		$f_1 = 0.29 \pm 0.06$, $\nu_{Q1} = 428 \pm 20$ MHz $\eta_1 = 0.34 \pm 0.08$, $\delta_1 = 0.022 \pm 0.0055$	Probe atoms associated with HfC
	Quenched Cu:Hf	$f_0 = 0.68 \pm 0.04$, $\langle \nu_0 \rangle = 0$	Probe atoms occupying substitutional sites
		$f_1 = 0.08 \pm 0.03$, $\nu_{Q1} = 428 \pm 22$ MHz $\eta_1 = 0.38 \pm 0.13$, $\delta_1 = 0.021 \pm 0.0056$	Probe atoms associated with HfC
		$f_2 = 0.10 \pm 0.03$, $\nu_{Q2} = 348 \pm 12$ MHz $\eta_2 = 0.35 \pm 0.11$, $\delta_2 = 0.016 \pm 0.0055$	Probe atom associated with HfC binding divacancy
		$f_3 = 0.14 \pm 0.04$, $\nu_{Q3} = 115 \pm 7$ MHz $\eta_3 = 0.29 \pm 0.14$, $\delta_3 = 0.0211 \pm 0.0066$	Probe atom associated with HfC binding monovacancy
Positron lifetime	Reference Cu:Hf	$\tau_1 = 115 \pm 5$ ps, $I_1 = 0.81 \pm 0.06$	Bulk lifetime
		$\tau_2 = 163 \pm 20$ ps	Positron annihilating at off-stoichiometric defects in HfC
	Quenched Cu:Hf	$\tau_1 = 120 \pm 5$ ps, $I_1 = 0.55 \pm 0.06$	
		$\tau_2 = 230 \pm 5$ ps, $I_2 = 0.45 \pm 0.07$	Annihilation at divacancy

of the Lorentzian distribution of quadrupole frequency ($\delta\nu_0$) is understood to be due to carbon contamination in the sample. The fraction f_1 is interpreted as being due to probe atoms associated with HfC precipitates. The quadrupole component corresponding to the probe atoms associated with Hf solute clusters represented by $\nu_Q = 290 \pm 4$ MHz as observed in the

case of carbon free Cu:Hf and Al:Hf [10, 11] samples is not observed in the present studies. This indicates that Hf solute clusters are either absent or present only in a very dilute concentration to be detected. The macro structure of HfC precipitates is fcc. As the nearest neighbour environment of the substitutional Hf atoms in the HfC precipitate is of cubic symmetry, the observed defect component in the reference sample as indicated by f_1 is plausibly interpreted to be due to the probe atoms occupying the near surface of the HfC precipitate. The results of positron lifetime measurements (cf table 1) in the reference sample show that τ_1 is around 115 ps. This is lower than the bulk positron lifetime of 120–125 ps in defect free Cu [28]. This is understood to be caused by the presence of other positron traps. The lifetime component τ_2 is identified to be due to the positrons annihilating at the off-stoichiometric point defects, preferably Hf vacancies in HfC precipitate. Details of positron lifetime measurements in metallic carbides can be referred to in the literature [29, 30].

Having studied the reference sample by both of these experiments, we will see the results on the quenched samples. The fitted anisotropy spectrum corresponding to the as quenched sample is shown as figure 2(b). The resultant parameters in the quenched sample are shown in table 1. Figure 2(c) shows the $R(t)$ spectrum obtained in the sample following the annealing treatment at 600 K. Data analysis indicates that there is a slight increase in the fraction f_3 to 0.16 ± 0.05. The other fractions are $f_0 = 0.64 \pm 0.05$, $f_1 = 0.08 \pm 0.02$ and $f_2 = 0.11 \pm 0.03$. The remaining quadrupole parameters such as quadrupole frequencies and the respective widths of their Lorentzian distributions and the asymmetry parameters are the same as those of the quenched sample as shown in table 1. TDPAC measurements indicate that there is little or no change in the quadrupole parameters for annealing treatments below 1200 K. Subsequent to annealing at 1300 K, it is seen that the defect associated fractions f_2 and f_3 are absent. The corresponding $R(t)$ spectrum is shown in figure 2(d). The following are the quadrupole parameters as deduced, namely $f_1 = 0.16 \pm 0.03$, $\nu_{Q1} = 433 \pm 10$ MHz, $\delta_1 = 0.035 \pm 0.013$ and $\eta_1 = 0.16 \pm 0.08$, which are similar to those experienced by the probe atoms occupying the surface of the HfC precipitates as observed in the reference sample. In the following we will argue that the vacancies are quite stable due to binding by HfC and not isolated Hf atoms in the sample. Also the plausible geometry of probe–vacancy complexes will be deduced.

Hafnium atoms occupying substitutional sites binding either a mono- or divacancy would experience quadrupole frequencies associated with a zero asymmetry parameter. Also, if Hf–V_1 (or Hf–V_2) complexes are presumed to be formed due to quenching, they would have been formed in a large concentration ($C_V \approx 2.08 \times 10^{-4}$) taking into account a high quenching rate (8.5×10^3 K s^{-1}) and the value of the monovacancy formation energy ($E_F = 1.13$ eV) [31]. The absence of defect components with appreciable values of the fractions and the associated near zero value of the asymmetry parameter rules out that the fractions f_2 and f_3 are due to isolated, substitutional hafnium atoms binding these defects. The resolved anistropy spectra corresponding to the quenched sample is shown in figure 3. Based on the TDPAC experimental results on vacancies in fcc systems, Collins *et al* [17] have deduced the geometry of the probe–vacancy complexes based on the computation of EFG and the asymmetry parameter by the point charge model. Based on this model we interpret that the fraction f_3 (115 MHz) is due to probe atoms associated with HfC binding monovacancies (cf the inset of figure 3(a)). The fraction f_2 (348 MHz) is interpreted to be due to probe atoms associated with HfC binding divacancies. The geometry of the probe–divacancy complex is shown in the inset of figure 3(b); it is characterized by a quadrupole frequency and hence electric field gradient (EFG) which is nearly 2.5 times that of the EFG due to a probe atom binding a single vacancy. This is only closer to the present result in which $\nu_{Q2}/\nu_{Q3} \approx 3$. The non-zero asymmetry parameter close to 0.3 associated with both fractions f_2 and f_3 is understood to be due to relaxation of the probe atom around the concerned defect complex. Further, the present case is also complicated due

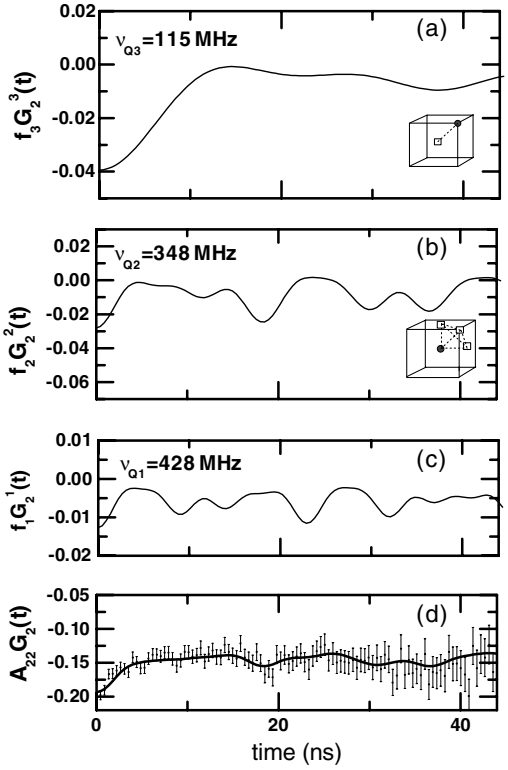

Figure 3. Resolved TDPAC spectra in the as-quenched Cu:Hf sample containing HfC solute clusters. The resolved fractions $f_1\,G_2^1(t)$, $f_2\,G_2^2(t)$ and $f_3\,G_2^3(t)$ are due to probe atoms associated with HfC solute clusters and HfC binding monovacancies and divacancies respectively. The inset shows the geometry of the corresponding probe–vacancy complexes based on the computation of EFG using the point charge model [16].

to the strain at the interface which is likely to affect the symmetry of the probe–defect complex. This experiment illustrates that HfC precipitates in Cu strongly bind small vacancies and hence resist the formation of large vacancy clusters and prevent void swelling in the Cu matrix.

The variation of the resolved positron lifetime parameters as a function of annealing temperature for the quenched sample is shown in figure 4. From these results on the quenched sample (cf table 1), it can be noted that the value of τ_2 is of the order of 230 ps. This is attributed to positron trapping at small vacancy clusters, plausibly a divacancy. It is interesting to notice that the corresponding intensity I_2, which is identified to be due to positron annihilation at vacancy clusters bound by HfC, remains a nearly constant behaviour until 1200 K, thereby indicating the high thermal stability of the vacancy clusters. The positron lifetime is predominantly dictated by the higher lifetime due to divacancy complexes. On comparing the positron lifetime results on the helium irradiated Cu:Hf sample [11], it is deduced that HfC precipitates bind vacancies with a higher binding energy than simple Hf solute clusters. As seen in figure 4 beyond 1200 K, τ_2 decreases to a value of 148 ± 1 ps. This is concomitant with the detrapping of vacancies from HfC precipitates as deduced by TDPAC measurements as discussed above. The removal of vacancies from HfC precipitates is understood to be due to diffusion of Hf from the matrix into the precipitate. The value of τ_2 ($\approx$148 ps) is different from that of the reference sample (163 ps). Also, it is seen that there

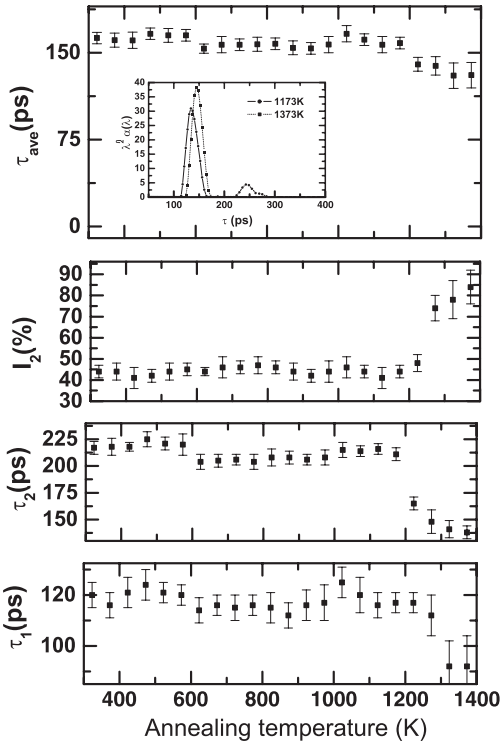

Figure 4. The variation of the resolved positron lifetime parameters in the quenched Cu:Hf sample with annealing temperature. The inset shows the computed values of the annihilation rate probability distribution function $\lambda^2\alpha(\lambda)$ versus τ for the sample subsequent to annealing treatments at 1173 and 1273 K.

is an increase in I_2 beyond 1200 K. Based on these parameters, it is interpreted that beyond 1200 K, which marks the vacancy detrapping temperature, poistrons predominantly annihilate at the surface of the precipitates. In the reference and quenched samples the annihilation of positrons was at off-stoichiometric carbides due to their strong affinity. Beyond 1200 K it is observed that there is a preferential annihilation of positrons at HfC precipitates themselves, due to a strong trapping of positrons at these precipitates.

Based on the annihilation rate probability distribution function $\lambda^2\alpha(\lambda)$ computed by CONTIN analysis, a few spectra of $\lambda^2\alpha(\lambda)$ versus $1/\lambda$ (i.e. τ) obtained for isochronal measurements at 1173 and 1373 K are shown as an inset of figure 4. In the sample annealed at 1173 K, there occur two peaks with mean values at around 140 and 240 ps respectively. The peak around 240 ps is quite wide and the distribution of positron lifetime is between 225 and 275 ps. Annealing at 1373 K leads to the disappearance of the peak around 240 ps and a single peak is observed around 140 ps which is of higher lifetime than that of the annealed reference sample. τ_2 in the reference sample is seen to be due to annihilation of positrons at off-stochiometric defects such as Hf vacancies and in the quenched sample it is understood to be due to annihilation at divacancies. Annealing beyond 1200 K almost results in the absence of strong trapping centres of positrons such as vacancies. This mainly results in annihilation at the surface of the precipitates. This case represents an increased concentration of trapping centres and hence leads to a dominant peak at 140 ps in the CONTIN plot which is also represented as an increase in I_2 in the lifetime results.

In summary, the combined TDPAC and positron lifetime measurements on the quenched Cu:Hf sample show that HfC precipitates bind quenched vacancies very strongly, with the detrapping of these defects occurring beyond 1200 K. We have not observed the presence of vacancy accretion leading to their clustering in these measurements, implying that the HfC precipitates bind vacancies/divacancies very strongly and resist the clustering of bigger vacancies and void swelling in the Cu matrix.

4. Conclusions

The Cu:Hf sample is observed to contain HfC precipitates as deduced by TEM and microdiffraction analysis. TDPAC and positron lifetime measurements carried out in the quenched sample show that these precipitates bind small vacancies very strongly. The detrapping of vacancies/divacancies from HfC precipitates is found to occur for annealing treatments beyond 1200 K, implying that HfC precipitates effectively resist the formation of higher vacancy clusters or voids in Cu matrix. Detailed studies on these systems with a controlled doping or introduction of metallic carbide clusters might unravel new and interesting results.

Acknowledgments

We would like to thank C S Sundar and G Amarendra for discussions and encouragement. Our sincere thanks are due to Mythili Govindaraj, Saroja Saibaba and Vijayalakshmi for TEM/ microdiffraction measurements. We thank the referees for their useful suggestions.

References

[1] Dederichs P H, Drittler B, Klemradt U and Zeller R 1992 *Mater. Sci. Forum* **105–110** 1
[2] Somoza A, Petkov M P, Lynn K G and Dupasquier A 2002 *Phys. Rev.* B **65** 094107
[3] Jhi S H, Ihm J, Louie S G and Cohen M L 1999 *Nature* **132** 152
[4] Jhi S H, Louie S G, Cohen M L and Ihm J 2001 *Phys. Rev. Lett.* **86** 3348
[5] Alam A and West R N 1982 *J. Phys. F: Met. Phys.* **12** 389
[6] Sielemann R 1987 *Mater. Sci. Forum* **15–18** 25
[7] Swanson M L, Howe L M, Qunneville A F, Wichert Th and Deicher M 1984 *J. Phys. F: Met. Phys.* **78** 1603
Also see Jackman J, Wichert Th and Swanson M L 1987 *J. Phys. F: Met. Phys.* **78** 1357
[8] Hautojarvi P 1979 *Positrons in Solids* (Berlin: Springer)
[9] Hautojarvi P 1987 *Mater. Sci. Forum* **15–18** 81
[10] Govindaraj R, Venugopal Rao G, Gopinathan K P and Viswanathan B 1999 *Pramana J. Phys.* **52** 219
[11] Govindaraj R, Gopinathan K P and Viswanathan B 2000 *Bull. Mater. Sci.* **23** 201
[12] Bloom E E, Stieger J O, Rowcliffe A O and Leitnaker J M 1976 *Scr. Metall.* **10** 303
[13] Bloom E E, Leitnaker J M and Steigler J O 1976 *Nucl. Technol.* **31** 232
[14] Kesternich W and Rothaut J 1981 *J. Nucl. Mater.* **103/104** 845
[15] Mazey D J, Harnies D R and Hudson J A 1980 *J. Nucl. Mater.* **89** 155
[16] Kimura A *et al* 2002 *J. Nucl. Mater.* **307** 521
[17] Collins G S, Shropshire L and Fans J 1990 *Hyperfine Interact.* **62** 1
[18] Pleiter F and Hohenemser C 1982 *Phys. Rev.* **25** 106
[19] Hautojarvi P, Heinio J, Manninen M and Nieminen R 1977 *Phil. Mag.* **35** 973
[20] Lynn K G *et al* 1977 *Phys. Rev. Lett.* **38** 241
[21] Govindaraj R and Gopinathan K P 1996 *J. Nucl. Mater.* **231** 141
Also see Govindaraj R and Rajaraman R 2000 *J. Phys.: Condens. Matter* **12** 5179
[22] Pleiter F, Venema W Z and Arends A R 1978 *Hyperfine Interact.* **4** 693
[23] Yates M L 1982 *Alpha, Beta and Gamma Ray Spectroscopy* vol 2, ed Siegbahn (Amsterdam: North-Holland) p 997
[24] Amarendra G, Viswanathan B, Rajaraman R, Srinivasan S and Gopinathan K P 1992 *Phil. Mag. Lett.* **65** 77

[25] Kirkegaard P, Eldrup M, Mogensen O E and Pedersen N J 1981 *Comput. Phys. Commun.* **23** 307
[26] Gregory R B 1991 *Nucl. Instrum. Methods* A **302** 496
Also see for example, Gregory R B 1991 *J. Appl. Phys.* **70** 4665
[27] Govindaraj R and Rajaraman R 1999 *Solid State Phys.* **42** 219
[28] Seeger A and Banhart F 1987 *Phys. Status Solidi* a **102** 171
[29] Puska M *et al* 1994 *Phys. Rev.* B **49** 10947
[30] Rampel A A *et al* 1993 *J. Phys.: Condens. Matter* **5** 261
[31] Doyama M and Koehler J S 1963 *Phys. Rev.* **127** 21